

# Formation Constants of Copper(II) Complexes with Tripeptides Containing Glu, Gly, and His: Potentiometric Measurements and Modeling by Generalized Multiplicative Analysis of Variance

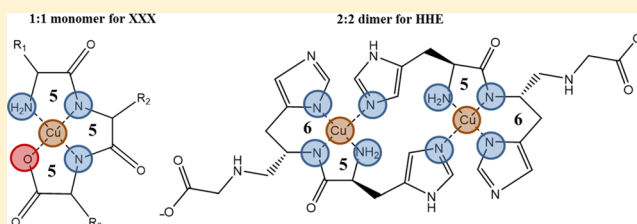
Rima Raffoul Khoury,<sup>†</sup> Gordon J. Sutton,<sup>†</sup> Diako Ebrahimi,<sup>‡</sup> and D. Brynn Hibbert<sup>\*,†</sup>

<sup>†</sup>School of Chemistry, UNSW Australia, Sydney NSW 2052, Australia

<sup>‡</sup>Centre for Vascular Research, Faculty of Medicine, UNSW Australia, Sydney NSW 2052, Australia

## S Supporting Information

**ABSTRACT:** We report a systematic study of the effects of types and positions of amino acid residues of tripeptides on the formation constants  $\log\beta$ , acid dissociation constants  $pK_a$ , and the copper coordination modes of the copper(II) complexes with 27 tripeptides formed from the amino acids glutamic acid, glycine, and histidine.  $\log\beta$  values were calculated from pH titrations with 1 mmol L<sup>-1</sup>:1 mmol L<sup>-1</sup> solutions of the metal and ligand and previously reported ligand  $pK_a$  values. Generalized multiplicative analysis of variance (GEMANOVA) was used to model the  $\log\beta$  values of the saturated, most protonated, monoprotonated,  $\log\beta(\text{CuL}) - \log\beta(\text{HL})$ , and  $pK_a$  of the amide group. The resulting model of the saturated copper species has a two-term model describing an interaction between the central and the C-terminal residues plus a smaller, main effect of the N-terminal residue. The model supports the conclusion that two copper coordination modes exist depending on the absence or presence of His at the central position, giving species in which copper is coordinated via two or three fused chelate rings, respectively. The GEMANOVA model for  $pK_{\text{amide}}$ , which is the same as that for the saturated complex, showed that Gly-Gly-His has the lowest  $pK_{\text{amide}}$  values among the 27 tripeptides. Visible spectroscopy indicated the formation of metal–ligand dimers for tripeptides His-His-Gly and His-His-Glu, but not for His-His-His, and the formation of multiple ligand bis complexes  $\text{CuL}_2$  and  $\text{Cu}(\text{HL})_2$  for tripeptides (Glu/Gly)-His-(Glu/Gly) and His-(Glu/Gly)-(Glu/Gly), respectively.



## INTRODUCTION

Peptides can be very efficient and very specific for binding a range of metal ions. The coexistence of different potential donor atoms in a peptide sequence allows the formation of complexes of different speciation and great variety of conformations (by changing steric and energetic constraints) for the same metal ion.<sup>1</sup>

Coordination chemistry of peptides has been studied since the early 1960s.<sup>1a,b,2</sup> An important key in metal coordination chemistry is the formation of stable 5- and/or 6-membered chelate rings through the N-terminal amino (which is often a primary  $-\text{NH}_2$  group except with proline where the amine group is secondary),<sup>1b</sup> C-terminal carboxylate, and side-chain donor groups if present.<sup>3</sup> The most important donor atoms of peptide side chains in terms of coordinating metal ions are the imidazolate-nitrogen of histidine, the thiolate-sulfur atom of cysteine, the carboxylate-oxygen of aspartic and glutamic acid, the amino-nitrogen of lysine, and the phenolic-oxygen of tyrosine. The amide nitrogen and carbonyl oxygen of peptide linkages can also coordinate metal ions<sup>1b</sup> but are less effective donor atoms than those in the terminal-amino and terminal-carboxylate groups.<sup>1a,4</sup> However, metal ions such as copper promote the deprotonation of the amide nitrogen of the peptide bond to form a very stable metal  $-\text{N}^-$  bond. For

example,  $\text{Cu}^{2+}$  can cause the deprotonation of the amide bond at pH 5.<sup>1a</sup>

Almost all metal ions present in the periodic table have been investigated, and their thermodynamic, kinetics, and structural properties are reasonably clarified.<sup>3a</sup> Among metal ions, copper(II) is the most studied because of its chemical and biological significance in proteins, enzymes, and various mechanisms such as peptide-folding processes and the biological functioning of peptides and proteins.<sup>1a–c,5</sup> Studies have shown that copper(II) ion has the same peptidic binding site at the N-terminus of human serum albumin HSA, which is its transfer route in the human body.<sup>4,5b,c</sup> Despite the large amount of research on various aspects of the copper coordination chemistry of peptides,<sup>1b,3b,6</sup> complete systematic studies in this area are lacking,<sup>2b</sup> and this was a motivation behind the present study.

The binding modes of tripeptide ligands can vary from peptide to peptide and are strongly influenced and controlled by the type and position of amino acid residues in the peptide sequences.<sup>1a,b</sup> Residues, particularly those with coordinating side chains, can interact to favor a particular conformation of

Received: April 17, 2013

the peptide, which defines the metal–peptide coordination thermodynamic and structural equilibria.<sup>1b</sup> These intramolecular interactions strongly influence the stability and conformation of the metallo-peptide complexes, thus affecting the biological functioning of peptides and proteins.<sup>1b</sup>

In our previous study we showed how the  $pK_a$  values of the 27 tripeptides composed of glutamic (Glu, E), glycine (Gly, G) and histidine (His, H) residues are influenced by the kind and position of residue in the peptide sequence.<sup>7</sup> In the present study we extend our investigation of the type and position of residues on the formation constants of copper(II) complexes with the same 27 tripeptide ligands.

The choice of amino acids Glu, Gly, and His was dependent on their biochemical properties. Glu has a carboxylate group side chain that acts as an additional potential donor atom for copper binding. This carboxylate side chain can also interact inter- and intramolecularly with other side-chain donor atoms (from Glu and His residues in this study). Glu has been shown to enhance the stability of 1N copper species (greater  $\log\beta$ ) when present in tripeptides. It decreases the  $pK_a$  of the preceding amide proton but increases  $pK_a$  of the consecutive amide proton. It allows the copper coordination to start at a more acidic pH and facilitates the formation of polyprotonated copper species.<sup>2i,8</sup> Gly is a flexible spacer; it is the shortest amino acid, and it does not have coordinating side chains.<sup>9</sup> Among amino acids, His has the strongest metal coordinating site due to the nitrogen of its imidazole ring side chain, and it is the most common binding site in metallo-proteins. His has a highly coordinating nitrogen atom in its imidazole ring which competes with the nitrogen of the terminal amine for the primary copper binding site. It can initiate the copper coordination when present in a tripeptide.<sup>2a–c,g,h,3a</sup> Although, the O-carboxylate side chain of Glu is a weak donor atom because of its presence at a gamma position from the peptide backbone, it can interact with the side chain of His. This interaction has not been completely understood.

The peptide series studied encompasses tripeptides which resemble motifs found in biological systems of interest, such as Asp-Ala-His-Lys (DAHK), the N-terminal sequence of human serum albumin (HSA), and Gly-His-Lys, the copper binding growth factor of plasma.<sup>5a,10</sup>

The equilibrium constants of complexation reactions are calculated from potentiometric titration measurements and then combined with  $pK_a$  values for the ligands (measured in our previous study)<sup>7</sup> to give  $\log\beta$  values for the new copper–ligand equilibria. The  $\log\beta$  literature values of the featured tripeptides and copper ions are given in the Supporting Information. We previously demonstrated that  $pK_a$  values of tripeptides may be modeled in terms of interactions between the amino acid residues using the multiway approach of generalized multiplicative analysis of variance (GEMANOVA). As metal peptide complexes involve interactions between the metal center and each residue, we expected and demonstrate in this paper that the  $\log\beta$  values of metal–peptide complexes can be similarly modeled by GEMANOVA. GEMANOVA models can be used to predict the measured responses at given instances of studied factors.<sup>11</sup> Therefore, predictions of unmeasured  $\log\beta$  and  $pK_a$  values in a series of peptides could be made using a subset of measured values taken from a suitably fractionated experimental design.

## ■ EXPERIMENTAL SECTION

**Experimental Design.** A full-factorial design was chosen to study the copper(II)-tripeptide complexes, with measurements of  $\log\beta$  made at every possible metal–ligand combination and over a range of pH values. The factors and the instances of each factor are the same as in our previous study.<sup>7</sup> The factors are the residue at the left, middle, and right positions of the tripeptide, arranged according to the IUPAC guidelines (N-terminal residue on the left-hand side and the C-terminal residue on the right-hand side), and the instances of each factor are Glu, Gly, or His. Therefore there are  $3^3 = 27$  possible combinations of tripeptides (see Scheme S1 in Supporting Information.)

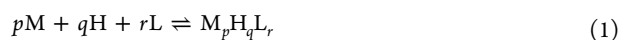
**Materials.** The 27 tripeptides (*EEE*, *EEG*, *EEH*, *EGE*, *EGG*, *EGH*, *EHE*, *EHG*, *EHH*, *GEE*, *GEG*, *GEH*, *GGE*, *GGG*, *GGH*, *GHE*, *GHG*, *GHH*, *HEE*, *HEG*, *HEH*, *HGE*, *HGG*, *HGH*, *HHE*, *HHG*, *HHH*) were obtained and used without further purification. Underlined tripeptides were bought from Sigma Aldrich (St Louis, MO) with purity greater than 98%. Those in italics were obtained from Bachem (Switzerland) with purity greater than 98%, and the remaining tripeptides were obtained from Genosphere Biotechnologies (France) as a trifluoroacetate salt with purity greater than 98% by TLC and HPLC. The peptides were freeze-dried before use and stored in a freezer at  $-20\text{ }^\circ\text{C}$ .

**Methods.** The potentiometric titration method employed followed that of Yokoyama<sup>12</sup> and was adapted from the IUPAC guidelines for apparatus,<sup>13</sup> measurement,<sup>14</sup> and critical evaluation of the reported equilibrium constants in aqueous solution.<sup>13,15</sup> Titrations were carried out on 10 mL solutions containing a ligand ( $1\text{ mmol L}^{-1}$ ), copper(II) ( $1\text{ mmol L}^{-1}$ ), and HCl ( $2\text{ mmol L}^{-1}$ ) with titrant aqueous sodium hydroxide ( $0.1002\text{ mol L}^{-1}$ ). Copper concentrations were verified by inductively coupled plasma optical emission spectroscopy (ICP-OES) measurements. Sodium hydroxide solution was added in  $5\text{ }\mu\text{L}$  increments with continuous magnetic stirring, and the pH was measured using a calibrated Beckman  $\phi$  34 pH-meter and Mettler Toledo electrode pH (0–14) after each increment. The temperature was maintained at  $25.0 \pm 0.2\text{ }^\circ\text{C}$ , and the ionic strength was maintained by  $0.1\text{ mol L}^{-1}$  sodium perchlorate solution. Nitrogen gas on top of the solution during the titration minimized the effect on pH of carbon dioxide, which is present in the ambient air.<sup>14</sup>

pH measurement was calibrated using buffer solutions of  $\text{pH } 4.01 \pm 0.02$  and  $7.00 \pm 0.02$  purchased from PST ProSciTech (Australia). The sodium hydroxide solution was standardized by titration with a standard potassium hydrogen phthalate solution (Ajax Finechem, analytical reagent of purity greater than 99.8%) or with a hydrochloric acid solution, which itself was standardized with either  $\text{Na}_2\text{CO}_3$  Anhydrous (Ajax Finechem, analytical reagent of purity greater than 99.8%) or  $\text{NaHCO}_3$  (Ajax Finechem, analytical reagent of purity greater than 99.8%). For each titration curve, 60–100 volume added/pH points were collected. Each titration was repeated at least twice. Quoted results for  $\log\beta$  values are the weighted means of the estimated  $\log\beta$  values, where the weighting was proportional to the reciprocal of the square of the standard uncertainty of a  $\log\beta$  value.

Visible absorption spectra were recorded under the same experimental conditions as the pH titrations for copper ligand systems containing His (nine systems). A 3 mL sample of solution in a plastic disposable cuvette was titrated and UV–visible (Schimadzu UV-2400PC Series, 300 – 800 nm) spectra were recorded after every addition of  $30\text{ }\mu\text{L}$  of standard NaOH  $0.1\text{ mol L}^{-1}$ . A background spectrum of a solution containing copper(II) ions at  $1\text{ mmol L}^{-1}$  and hydrochloric acid HCl at  $2\text{ mmol L}^{-1}$  (in the absence of ligand) was recorded under the same experimental conditions.

**Data Analysis.** For a given tripeptide ligand the cumulative formation constants,  $\log\beta_{pqr}$ , of the complexes were calculated using the software HyperQuad 2008<sup>16</sup> according to the equilibrium equation (eq 1) and eq 2



$$\beta_{pqr} = \frac{[M_p H_q L_r]}{[M]^p [H]^q [L]^r} \quad (2)$$

where M is metal, H proton, and L ligand fully deprotonated in the metal-free system (when metal is present, further deprotonation of amide protons can occur). The simultaneous equations in concentrations of all complexes and free species are solved to give values of  $\log\beta_{pqr}$  that minimize the squares of the residuals between modeled and measured pH. Although our experimental conditions, with a metal–ligand ratio of 1:1 and relatively low concentrations (1 mmol L<sup>-1</sup>), favors 1:1 complexes, evidence for species such as bis complexes 1:2 and dimers 2:2 were found at mole fractions less than 5%. Thus, in eqs 1 and 2,  $p = 1$  and  $r = 1$ ,  $p = 1$  and  $r = 2$ , or  $p = 2$  and  $r = 2$  for the work presented here. The number of hydrogens lies between  $q = -3$  (both amide protons lost and one from a side-chain His) and  $q = 3$ , depending on the residues in the tripeptide. The justification for including only 1:1, 1:2, and 2:2 M:L complexes in the HyperQuad fitting is discussed in detail below.

$\log\beta$  values were estimated from the titration data by HyperQuad 2008 software. Data that were subject to greater error or gave little information about  $\log\beta$  values, from the beginning, end, and inflection point regions of the titration, were excluded from the refinement.<sup>16,17</sup> The inputs to HyperQuad are the titration data (titrant volume, pH), formulas of species to include in the model, initial concentrations and volume, temperature, and information for the uncertainty budget. The initial set of complexes included all possible copper–ligand species (when the ligand is fully protonated up to when the ligand is fully deprotonated, including the amide group deprotonation) that can be formed at a 1:1 metal-to-ligand ratio, 1:2 for HXX and XHX where X = E, G, H, and 2:2 for HHG and HHE. The output of the program are values of  $\log\beta_{pqr}$  with standard uncertainty values estimated from the covariance matrix of the residuals of the fitted values and information supplied by the user on uncertainties of volumetric apparatus, concentration, and purity of reagents and error in pH readings.<sup>16</sup> As any pK value can be expressed as the difference of successive  $\log\beta$  values, the standard uncertainty for the reported pK<sub>a</sub> values can be calculated as  $u(pK_{a,n}) = (u(\log(\beta_n))^2 + u(\log(\beta_{n-1}))^2)^{1/2}$ , assuming  $\text{Cov}(\log(\beta_n), \log(\beta_{n-1})) = 0$ . The implementation of the HyperQuad program was validated on data sets supplied with the software.

The theory of GEMANOVA was described in our previous work.<sup>7</sup> GEMANOVA is suitable for analyzing complex systems where the variation is mostly due to interactions between factors. Briefly, the log(equilibrium constant) for amino acids  $i$ - $j$ - $k$  ( $i = \text{E,G,H}$ ;  $j = \text{E,G,H}$ ;  $k = \text{E,G,H}$ ) was modeled as

$$X_{ijk} = a_i b_j c_k + d_i e f_{jk} + \varepsilon_{ijk} \quad (3)$$

where each term is a contribution of the particular amino acid at the given position and  $\varepsilon_{ijk}$  is a normally distributed residual. The modeling also allows any term in eq 3 to be made a constant ( $a_E = a_G = a_H = 1$ ,  $b_E = b_G = b_H = 1$ , etc.), which signifies that the position does not contribute to the model.

“Leave-one-out” cross-validation was used to estimate the error of a model and as a guide to choose between alternative models. Selection of the best model was based on the values of the root-mean-square errors of cross validation RMSECV defined as:

$$\text{RMSECV} = \sqrt{\frac{\sum_{i=1}^n (\hat{y}_i - y_i)^2}{n}} \quad (4)$$

for  $n$  data, where  $y_i$  is the measured value of datum  $i$  and  $\hat{y}_i$  is its estimated value when datum  $i$  has been removed from the model fitting. The model that returns the lowest RMSECV value was selected as the best model. When two or more models returned similar RMSECV values, the model with the fewest parameters was chosen.

GEMANOVA modeling was implemented in MATLAB, Version 2011a (The MathWorks Inc.). GEMANOVA MATLAB code was obtained from R. Bro. The GEMANOVA code was validated using data generated from known parameters.

## RESULTS

**Measurement of  $\log\beta$  Values.** Examples of measured and fitted pH titration curves for copper complexes of the tripeptides EEH, GHE, HEE, and HHH are shown in Figure 1. Each of the 27 titration curves is given in the Supporting Information.

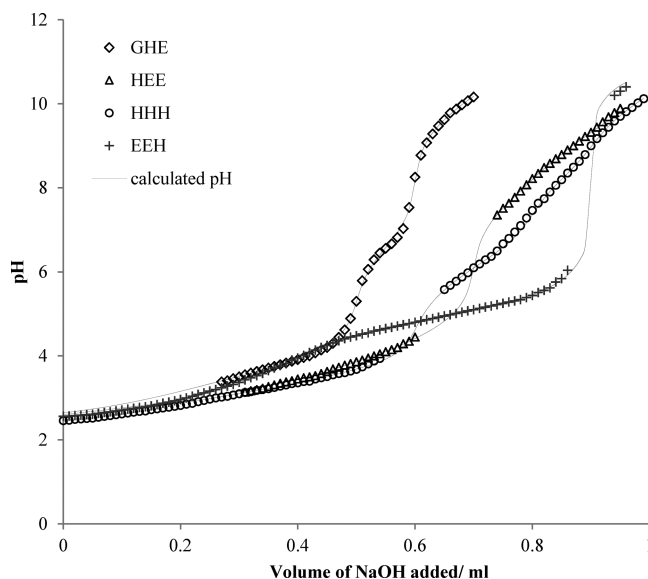


**Figure 1.** Example of titration curves for copper complexes with tripeptides EEH (+), GHE (◇), HEE (△), and HHH (○). Starting solution: 10 mL of a solution of concentrations 1 mmol L<sup>-1</sup> Cu<sup>2+</sup>, 1 mmol L<sup>-1</sup> tripeptide, and 2 mmol L<sup>-1</sup> HCl titrated with 0.1002 mol L<sup>-1</sup> NaOH. The solid lines are fitted by HyperQuad.

Table S1 in the Supporting Information summarizes the means, weighted inversely proportionally to their respective squared uncertainties, of the estimated  $\log\beta_{lqr}$  and pK<sub>a</sub> values of copper complexes with 27 tripeptides. pK<sub>a</sub>(CuL) is the pK<sub>a</sub> of the first amide proton to be lost, and pK<sub>a</sub>(CuH<sub>2</sub>L) is the pK<sub>a</sub> of the second amide proton to be lost. In other papers these have been termed pK<sub>1</sub> (amide) and pK<sub>2</sub> (amide), respectively.<sup>2i,18</sup> The value of  $\log\beta(\text{CuL}) - \log\beta(\text{HL})$  is also calculated to allow comparison of the underlying stability of the metal complexes without the effects of ligand acidity. In refs 2i and 18 this difference is written  $\log\beta(\text{CuL}) - \text{pK}_{\text{amino}}$ . Table 1 contains  $\log\beta_{lq1}$  and pK<sub>a</sub> values for the complexes in which the copper equatorial plane is most occupied or saturated by the ligand donor atoms (CuH<sub>sat</sub>L). A tripeptide containing His at position 2 raises the pK<sub>a</sub> of the second amide group and suppresses its deprotonation. As a consequence, for these ligands copper is ligated to the peptide via three bonds in the equatorial plane as CuH<sub>2</sub>L. The fourth equatorial position can be occupied by an oxygen atom of a water molecule or another ligand from a neighboring complex. For tripeptides that do not have His at the central position, both amide groups can be deprotonated. As a consequence, the copper is tetra-bound to the ligand in the equatorial plane as CuH<sub>2</sub>L.

**Visible Spectra.** Visible spectra were recorded and analyzed for His-containing ligands to obtain evidence for the formation of dimers or other polynuclear or multiligand complexes. Figure 2 shows spectra of complexes with GHE (only 2 components, no dimerization) and HHE, which has 3 components including a dimer M<sub>2</sub>L<sub>2</sub>. Also shown is the PCA decomposition with extracted spectra. Detailed results for ligands HHE, HHH,

Table 1.  $\log\beta_{1q1}$  and  $pK_a$  Values, with Standard Measurement Uncertainties, of Copper Complexes  $\text{CuH}_{\text{sat}}\text{L}$  with 27 Tripeptides<sup>a</sup>

tripeptide	$\text{CuH}_{\text{sat}}\text{L}$	$\log\beta$	$u(\log\beta)$	$pK_{\text{amide}}$	$pK_a$	$u(pK_a)$
EEE	$[\text{CuH}_{-2}\text{L}]$	-3.635	0.034	$pK_a(\text{CuH}_{-1}\text{L})$	6.295	0.052
EEG	$[\text{CuH}_{-2}\text{L}]$	-3.327	0.019	$pK_a(\text{CuH}_{-1}\text{L})$	6.992	0.025
EEH	$[\text{CuH}_{-2}\text{L}]$	1.120	0.026	$pK_a(\text{CuH}_{-1}\text{L})$	5.630	0.042
EGE	$[\text{CuH}_{-2}\text{L}]$	-5.198	0.029	$pK_a(\text{CuH}_{-1}\text{L})$	7.716	0.036
EGG	$[\text{CuH}_{-2}\text{L}]$	-2.406	0.020	$pK_a(\text{CuH}_{-1}\text{L})$	7.366	0.025
EGH	$[\text{CuH}_{-2}\text{L}]$	1.115	0.045	$pK_a(\text{CuH}_{-1}\text{L})$	5.285	0.060
EHE	$[\text{CuH}_{-1}\text{L}]$	12.627	0.059	$pK_a(\text{CuL})$	4.921	0.084
EHG	$[\text{CuH}_{-1}\text{L}]$	8.326	0.005	$pK_a(\text{CuL})$	4.890	0.007
EHH	$[\text{CuH}_{-2}\text{L}]$	3.381	0.065	$pK_a(\text{CuH}_{-1}\text{L})$	7.513	0.083
GEE	$[\text{CuH}_{-2}\text{L}]$	-2.096	0.056	$pK_a(\text{CuH}_{-1}\text{L})$	6.22	0.08
GEG	$[\text{CuH}_{-2}\text{L}]$	-5.091	0.066	$pK_a(\text{CuH}_{-1}\text{L})$	6.41	0.09
GEH	$[\text{CuH}_{-2}\text{L}]$	-6.347	0.070	$pK_a(\text{CuH}_{-1}\text{L})$	10.454	0.073
GGE	$[\text{CuH}_{-2}\text{L}]$	-5.458	0.012	$pK_a(\text{CuH}_{-1}\text{L})$	6.583	0.018
GGG	$[\text{CuH}_{-2}\text{L}]$	-5.827	0.026	$pK_a(\text{CuH}_{-1}\text{L})$	6.388	0.031
GGH	$[\text{CuH}_{-2}\text{L}]$	-0.736	0.044	$pK_a(\text{CuH}_{-1}\text{L})$	4.368	0.085
GHE	$[\text{CuH}_{-1}\text{L}]$	8.065	0.020	$pK_a(\text{CuL})$	9.813	0.040
GHG	$[\text{CuH}_{-1}\text{L}]$	6.459	0.081	$pK_a(\text{CuL})$	3.805	0.091
GHH	$[\text{CuH}_{-2}\text{L}]$	0.855	0.100	$pK_a(\text{CuH}_{-1}\text{L})$	7.420	0.139
HEE	$[\text{CuH}_{-2}\text{L}]$	-4.367	0.032	$pK_a(\text{CuH}_{-1}\text{L})$	8.966	0.041
HEG	$[\text{CuH}_{-2}\text{L}]$	-2.988	0.016	$pK_a(\text{CuH}_{-1}\text{L})$	8.558	0.020
HEH	$[\text{CuH}_{-2}\text{L}]$	0.968	0.032	$pK_a(\text{CuH}_{-1}\text{L})$	7.299	0.034
HGE	$[\text{CuH}_{-2}\text{L}]$	-3.478	0.048	$pK_a(\text{CuH}_{-1}\text{L})$	8.769	0.052
HGG	$[\text{CuH}_{-2}\text{L}]$	-5.450	0.039	$pK_a(\text{CuH}_{-1}\text{L})$	8.582	0.044
HGH	$[\text{CuH}_{-2}\text{L}]$	0.350	0.009	$pK_a(\text{CuH}_{-1}\text{L})$	6.324	0.015
HHE	$[\text{CuH}_{-1}\text{L}]$	10.902	0.056	$pK_a(\text{CuL})$	6.403	0.061
HHG	$[\text{CuH}_{-1}\text{L}]$	8.198	0.049	$pK_a(\text{CuL})$	5.962	0.060
HHH	$[\text{CuH}_{-2}\text{L}]$	-0.598	0.013	$pK_a(\text{CuH}_{-1}\text{L})$	7.856	0.023

<sup>a</sup>L represents the ligand with deprotonated carboxylate, imidazole and ammonium groups.  $\text{H}_{-1}\text{L}$  and  $\text{H}_{-2}\text{L}$  refer to tripeptides where one and two amide linkages have been deprotonated, respectively.

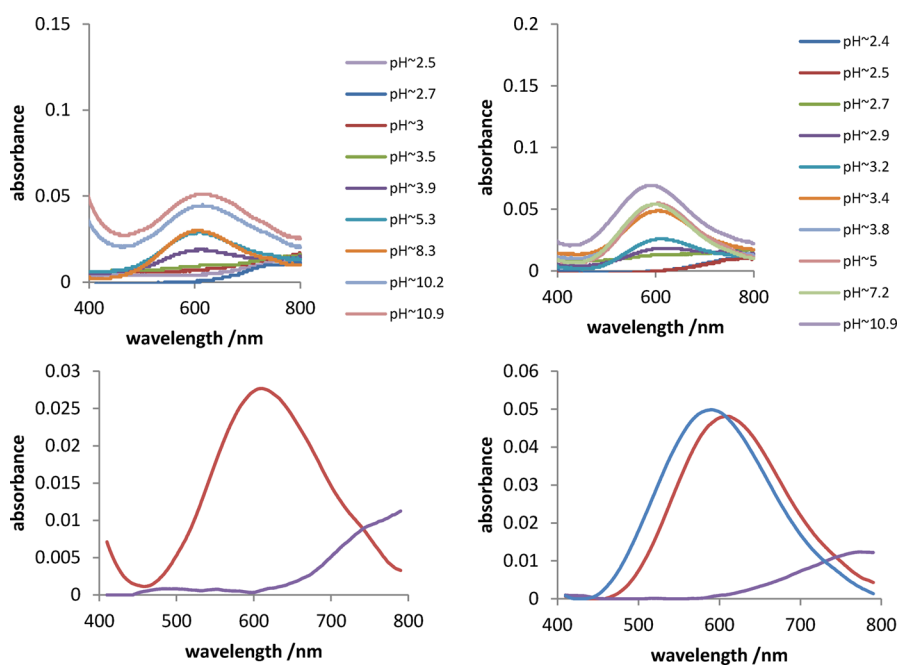


Figure 2. Top: visible spectra of 1 mmol  $\text{L}^{-1}$   $[\text{Cu}^{2+}]$  and 1 mmol  $\text{L}^{-1}$  ligand during titration by 0.1 mol  $\text{L}^{-1}$  NaOH. Bottom: spectra of components extracted by PCA and alternating constrained regression. Left column, ligand GHE; right column, ligand HHE.

GHE, and HGH are given in Supporting Information. A background shift in the visible spectra can be observed at high pH; this can be attributed to the precipitation of copper as

copper hydroxide and demonstrates that multiligand complexes such as  $\text{CuL}_2$  and  $\text{Cu}(\text{HL})_2$  bis complexes have been formed with  $\text{H}(\text{E}/\text{G}/\text{H})(\text{E}/\text{G}/\text{H})$  and  $(\text{E}/\text{G}/\text{H})(\text{E}/\text{G}/\text{H})$  ligands.



The species identified in the spectra of His-containing complexes are summarized in Table 2.

**Table 2. Analysis of Visible Spectra by Principal Components Analysis and Alternating Constrained Regression of His-Containing Complexes**

ligand	number of components in visible spectrum	wavelength maxima and identification <sup>a</sup>
HHX, X = E, G	3	580 nm 3N 2:2, 610 nm 3N 1:1, 770 nm Cu <sup>2+</sup> (aq)
HHH	3	520 nm 4N 1:1, 600 nm 3N 1:1, 770 nm Cu <sup>2+</sup> (aq)
HXH, X=E,G	3	520 nm 4N 1:1, 690 nm 2N 1:1, 790 nm Cu <sup>2+</sup> (aq)
XHY, X,Y = E,G	2	610 nm 3N 1:1, 790 nm Cu <sup>2+</sup> (aq)

<sup>a</sup>2N, 3N, and 4N are the number of coordinating nitrogen atoms.

**Analysis by GEMANOVA.** Log $\beta$  values modeled by GEMANOVA were of the following complexes: CuH<sub>sat</sub>L, in which the copper equatorial plane is most occupied or saturated by the ligand donor atoms (Table 1); most protonated complexes (CuH<sub>max</sub>L = CuH<sub>3</sub>L, CuH<sub>2</sub>L, or CuHL); monoprotonated (CuHL) and log $\beta$ (CuL) – log $\beta$ (HL). The models have terms of the form  $a_i b_j c_k$ , where  $a_i$  ( $i = E, G, \text{ or } H$ ) is the parameter for the N-terminal residue,  $b_j$  ( $j = E, G, \text{ or } H$ ) the parameter for the middle residue, and  $c_k$  ( $k = E, G, \text{ or } H$ ) the parameter for the C-terminal residue. In a model, each parameter may be held constant, giving a main effect (for single positions with two parameters constant) or an interaction effect between two positions (second-order effects with one parameter constant). The possible 37 different models comprising one and two terms were evaluated. No three-term models were tested as we have previously demonstrated that including a third term in the model gave no significant improvement to the fitting at the expense of a greater number of parameters estimated and required much longer computer times for convergence.<sup>7</sup> Tables S2–S6 in the Supporting Information contain details of all the models tested for the various copper species.

The best model selected in this paper for the CuH<sub>sat</sub>L has a two-term model describing an interaction between the central and the C-terminal residues plus an isolated main effect of the N-terminal residue. The model equation is

$$(\log \beta_{i,j,k})_{ijk} = a_i + e_j f_k \quad (i = E, G, H; j = E, G, H; k = E, G, H) \quad (5)$$

The values of the parameters are shown graphically in Figure 3. The log $\beta$  values calculated from the GEMANOVA model are plotted against the measured values in Figure 4. The error bars in the  $x$ -direction are  $2 \times u(\log \beta)$  from Table 1. The error bars for the calculated values were estimated from a bootstrapping exercise in which 100 random experimental sets were generated from the spread of replicated log $\beta$ . The error bar is the 95% confidence interval on the mean modeled log $\beta$  value.

## DISCUSSION

**Choice of Species to Consider in Titration and Modeling.** In the absence of His, Cu coordination starts at the N-terminus amino nitrogen, but when the peptide contains His, Cu coordination can also start at the imidazolate nitrogen on any His side chain. A large number of conformers can be formed for the mononuclear species depending on the steric

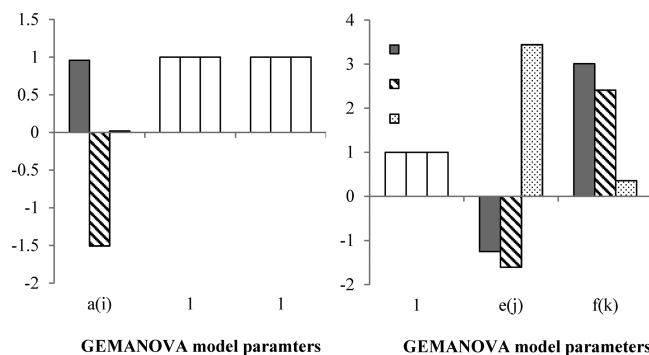


**Figure 3.** Parameters of the GEMANOVA model  $\log \beta(\text{CuH}_{\text{sat}}\text{L})_{ijk} = a_i + e_j f_k$ , eq 5. Solid bar, Glu (E); striped bar, Gly (G); dotted bar: His (H).

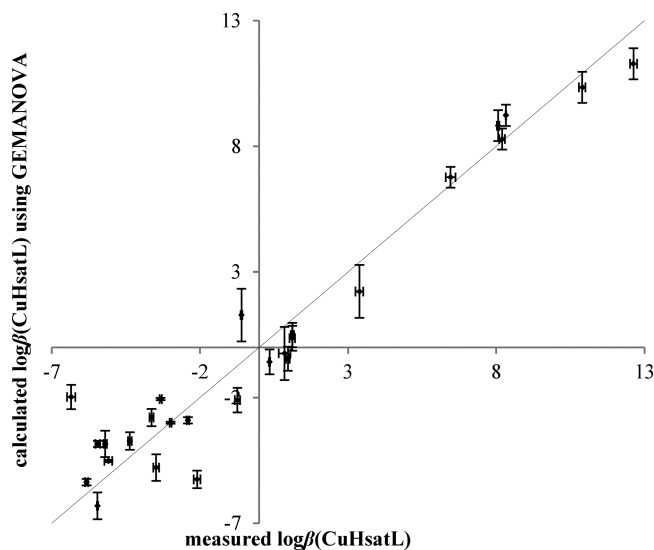


**Figure 4.** Plot of log $\beta$  of CuH<sub>sat</sub>L estimated by the GEMANOVA model given in eq 5 versus measured log $\beta$ . Horizontal error bars are  $\pm 2u(\log \beta)$ , and the vertical error bars are  $\pm 2s(\log \beta)$  obtained from the bootstrapping procedure.

and hydrophobic effect of the noncoordinating side chain.<sup>1a,b,2,3</sup> His residues of a peptide can act as independent metal binding sites (when well-separated) and can coordinate as many Cu<sup>2+</sup> as the number of His to facilitate the formation of polynuclear species.<sup>3a</sup> As such, only ligands containing two or more His residues can form polynuclear species, (M:L =  $n:1$ ), where  $n$  is the number of His + 1.

The dinuclear species Cu<sub>2</sub>L was introduced into the modeling of log $\beta$  values of HEH, HGH, and HHH. The insertion of the new species (2:1) caused problems with convergence, requiring up to 70% of the points to be excluded from the refinement. The fitting was not improved, and log $\beta$  values of the 1:1 species were not changed by more than 2%. This is discussed in the HyperQuad manual as indicating the introduction of a superfluous species. We suspect that at high pH this species might be produced but in too low a concentration to be picked out by the fitting of the titration.

His in a peptide creates the strongest ligand field, and as such, 1: $n$  (M:L) complexes involving His are more likely to be formed, and will be more stable when formed, than when His is not present. Complexes containing His can polymerize via relatively strong imidazolate bridges, whereas complexes without His (i.e., containing only Glu or Gly) form weaker

**Scheme 1.** Coordination Schemes for CuL Monomer Obtained with a Tripeptide without His (left panel) and the 2:2 Dimer with His-His-Glu (right panel)

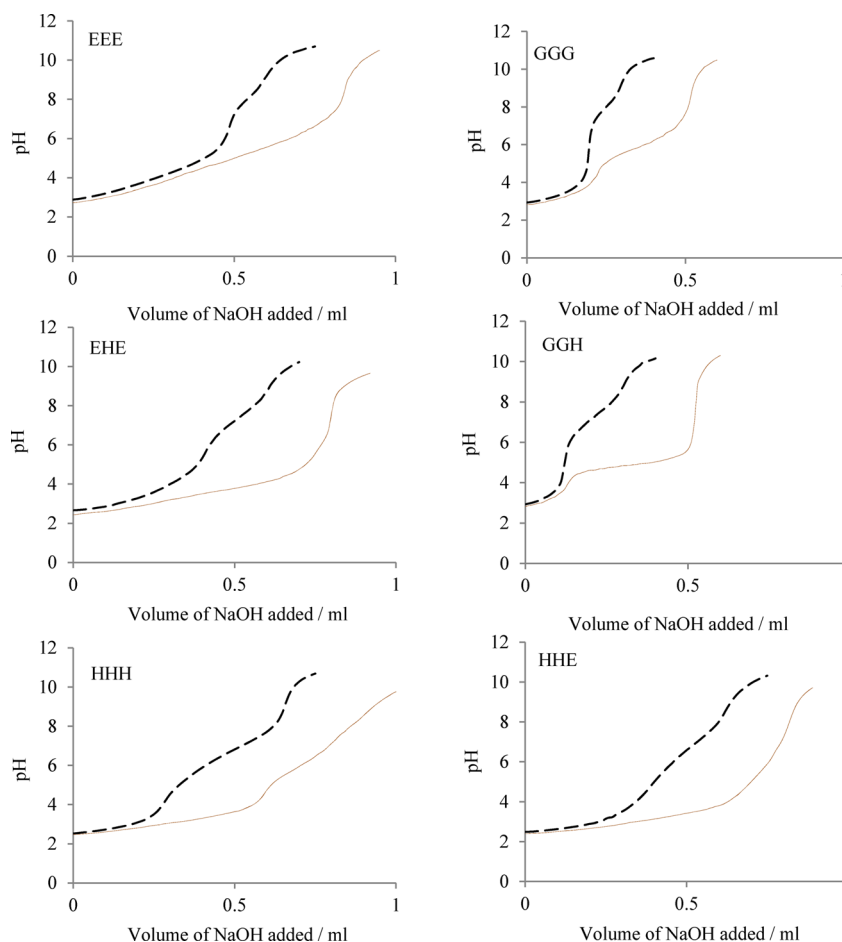
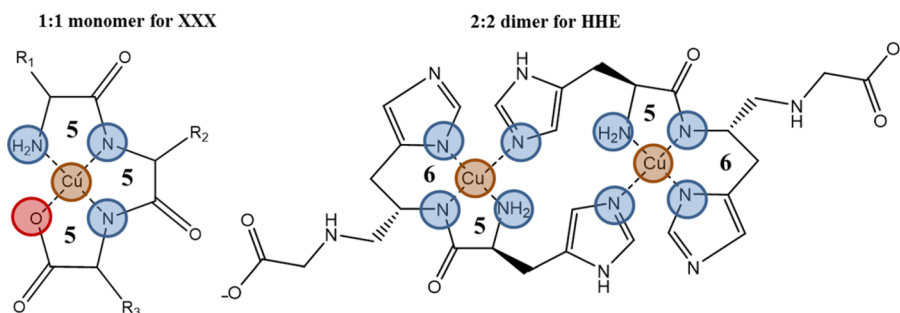


**Figure 5.** Titration curves for tripeptides EEE, GGG, EHE, GGH, HHH, and HHE, from left to right and top to bottom in the absence (dashed lines) and presence of copper (solid brown lines); 10 mL of Cu<sup>2+</sup> (1 mmol L<sup>-1</sup>) + tripeptide (1 mmol L<sup>-1</sup>) + HCl (2 mmol L<sup>-1</sup>) titrated with NaOH (0.1002 mol L<sup>-1</sup>).

$n:n$  bridges, at best. Previous studies on peptides containing His have shown the formation of bis complexes Cu(HL)<sub>2</sub> and CuL<sub>2</sub> when His is at the N-terminus and position 2 of a tripeptide and the formation of dimers 2:2 as (CuH<sub>1</sub>L)<sub>2</sub> species for peptides containing His at position 2.<sup>2b,g,12,19</sup> As with  $n:1$  species, we found that titration points were required to be excluded from the new fitting to attain convergence when 1:2 species were introduced. For (E/G)H(E/G), the bis complexes formed had formulas CuL<sub>2</sub> and were formed at a maximum of 5% for GHG at pH 4.3. Our results are in agreement with the findings of Farkas et al.<sup>20</sup> and Aiba et al.,<sup>19d</sup> who reported the formation of low percentages of such complexes. The

tripeptides H(E/G/H)(E/G/H) mainly formed bis complexes of formulas Cu(HL)<sub>2</sub> (apart from HGG which formed CuL<sub>2</sub>). For (E/G)H(E/G), CuL<sub>2</sub> was the bis complex formed. This can be attributed to the presence of His at position 2, which facilitates the deprotonation of the first amide group at acidic pH but hinders the deprotonation of the second amide group up to a high pH.

Previous research that reported dimer species 2:2 for peptides containing His at position 2 found a shift in the peak absorption wavelength of about 50 nm (from 600 nm for 1:1 species to 555 nm for 2:2 species) within the visible spectrum at high pH. Evidence in the visible spectra (peak at

around 580 nm in addition to the 1:1 peak at 620 nm) supports the presence of dimers for ligands HHG and HHE, for which the 3N coordination does allow dimerization. We therefore considered the series of dimers  $\text{Cu}_2(\text{His-His-Gly})_2$  and  $\text{Cu}_2(\text{His-His-Glu})_2$  for fitting the titration curves and subsequent GEMANOVA modeling. A peak at the low 500 nm is also expected from complexes that have a 4N coordination sphere. This is seen for H(E/G)H at around 520 nm, and 4N coordination precludes dimer formation. A coordination schematic representation for the 2:2 dimeric species obtained only when two His are present versus the 1:1 monomeric species obtained with ligands lacking the His residue is given in Scheme 1.

With (E/G/H)(E/G)(E/G/H) tripeptide ligands, copper is coordinated to the ligand donor atoms through its four equatorial positions. This leads to saturation of the copper equatorial plane and not leaving any of the equatorial site to bind to donor atoms from another neighboring ligand molecule. Whereas with HH(E/G), only three equatorial positions are occupied by the donor atoms of a same ligand molecule, thus allowing readily available donor atoms from the medium to occupy the fourth equatorial position; as a consequence, a His at N-terminus from another neighboring molecule can create a bridge to this fourth equatorial site and saturate the copper coordination equatorial plane.

**Titration Curves.** Example titration curves for the tripeptides EEE, GGG, HHE, EHE, GGH, and HHH in the absence and presence of copper are shown in Figure 5 to illustrate the range of behaviors found.

Once copper is bound to the tripeptide it will facilitate the deprotonation of labile protons, resulting in a titration curve that is lower than that in the absence of copper. The divergence of each ligand's pair of titration curves in the presence and absence of metal ions indicates significant extent of complexation. The pH at which the curves diverge was greater than 4.0 for EEE, GGG, and GGH but less than 3.0 for EHE, HHE, and HHH, which indicates for the latter group a greater sensitivity and an ability to capture copper ions in more acidic media.

**log $\beta$  Values.** The values of log $\beta$  may be understood in terms of the expected binding in the different tripeptides. For ligands containing multiple H and E residues, multiprotonated copper species are expected to be formed with higher log $\beta$  values compared to others.<sup>2g,i</sup> The percentages of free copper at pH 3, 7, and 10 were calculated and confirmed this observation. The values are shown in Table 3. HHE showed low free copper percentages at the three different pH values, indicating its potential application for copper sequestration and sensing.

**Interpretation of Modeling.** The selected GEMANOVA model for log $\beta$  of  $\text{CuH}_{\text{sat}}\text{L}$  (eq 5, figure 3) has two terms; an interaction between the central and the C-terminal residues and a smaller main effect of the N-terminal residue. The interaction term determines most of the log $\beta$  values; choosing only this term still fits the data adequately. His at the central position always gives a positive contribution to the log $\beta$  values, while Glu and Gly lead to negative contributions. The model predicts that Glu-His-Glu has the greatest log $\beta$  for  $\text{CuL}_{\text{sat}}$  ( $\text{CuH}_{-1}\text{L}$ ), which is supported by experiment. Table 3 similarly shows that Glu-His-Glu has the lowest free copper percentage at pH 7 and the second lowest, after Glu-His-His, at pH 10. This interpretation of the model suggests that different copper coordination processes occur depending on whether His is present or absent at the central position. Examples of the

**Table 3. Calculated Mole Fractions (Expressed as Percentages) of Free  $\text{Cu}^{2+}$  at pH 3, 7, and 10 in a Solution Containing 1 mmol  $\text{L}^{-1}$   $\text{Cu}^{2+}$  and 1 mmol  $\text{L}^{-1}$  Tripeptide<sup>a</sup>**

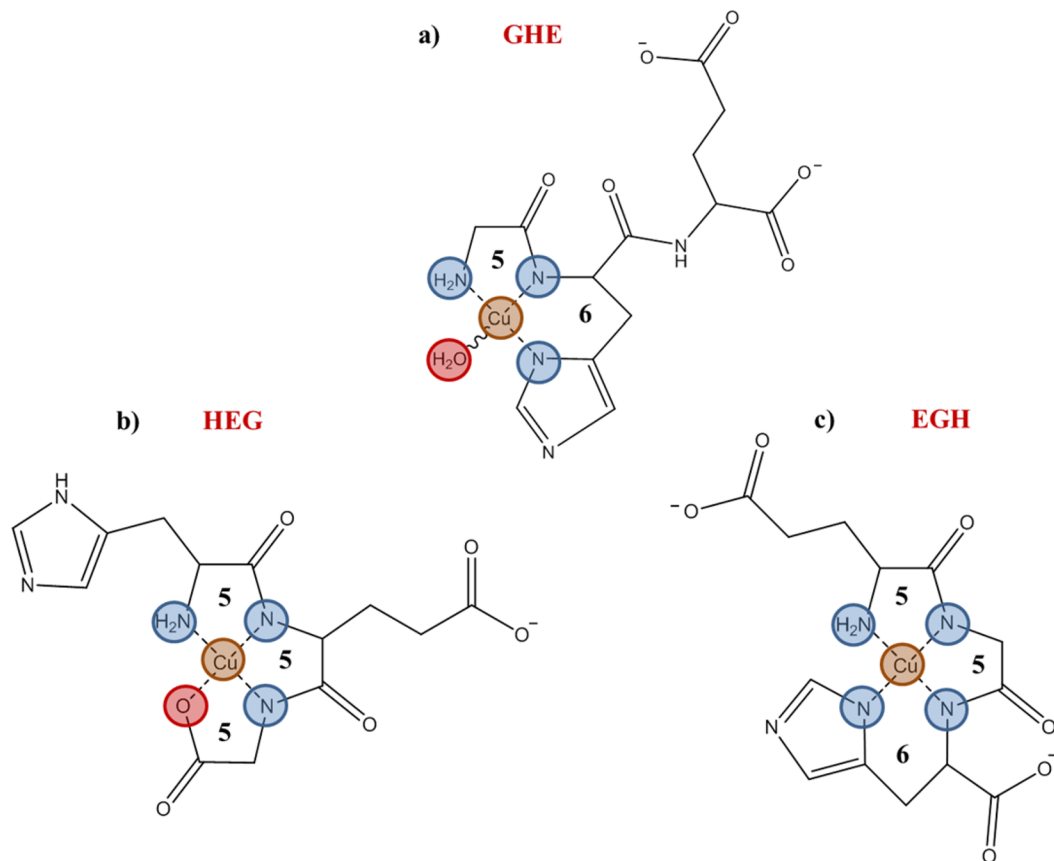
tripeptide	pH 3	pH 7	pH 10
EEE	72	0.13	$5.50 \times 10^{-6}$
EEG	88	0.15	$1.52 \times 10^{-5}$
EEH	86	$7.5 \times 10^{-3}$	$8.67 \times 10^{-8}$
EGE	71	0.36	$1.05 \times 10^{-4}$
EGG	80	0.045	$4.91 \times 10^{-6}$
EGH	(22) <sup>a</sup>	$3.0 \times 10^{-3}$	$6.60 \times 10^{-8}$
EHE	49	$1.3 \times 10^{-5}$	$9.31 \times 10^{-9}$
EHG	75	$5.7 \times 10^{-4}$	$1.31 \times 10^{-6}$
EHH	63	$6.5 \times 10^{-5}$	$4.06 \times 10^{-9}$
GEE	81	0.030	$3.04 \times 10^{-7}$
GEG	86	0.37	$5.19 \times 10^{-5}$
GEH	100	0.032	$2.52 \times 10^{-4}$
GGE	94	0.56	$1.77 \times 10^{-4}$
GGG	n.a.	0.46	$1.39 \times 10^{-4}$
GGH	98	$4.9 \times 10^{-4}$	$7.18 \times 10^{-7}$
GHE	96	0.015	$5.73 \times 10^{-6}$
GHG	74	$7.5 \times 10^{-3}$	$9.08 \times 10^{-6}$
GHH	47	$5.8 \times 10^{-4}$	$1.23 \times 10^{-7}$
HEE	73	1.61	$5.21 \times 10^{-5}$
HEG	77	0.050	$7.00 \times 10^{-6}$
HEH	56	$2.4 \times 10^{-3}$	$1.70 \times 10^{-7}$
HGE	53	0.013	$6.00 \times 10^{-6}$
HGG	58	2.48	$1.17 \times 10^{-4}$
HGH	63	$9.2 \times 10^{-4}$	$1.60 \times 10^{-7}$
HHE	32	$6.8 \times 10^{-5}$	$2.53 \times 10^{-8}$
HHG	74	$2.0 \times 10^{-4}$	$6.70 \times 10^{-7}$
HHH	63	0.12	$2.84 \times 10^{-7}$

<sup>a</sup>Values in parentheses are not considered reliable.

structures arising from these processes, for GHE, EGH and HEG, are shown in Scheme 2a–c.

Coordination of Cu(II) to the (E/G)H(E/G) and (E/G)(E/G)H peptides are strongly reminiscent of the Cu(II) coordination to the two naturally occurring peptide copper chelators, Gly-His-Lys (GHK), the copper binding growth factor of plasma,<sup>21</sup> and Asp-Ala-His-Lys (DAHK), the N-terminal coordination residues of human serum albumin HSA, whose X-ray structures showed geometry similar to those reported in Scheme 2a,c.<sup>10b,21,22</sup> The X-ray structures reported by Hureau et al.<sup>10b</sup> of GHK and DAHK showed that  $\text{Cu}^{2+}$  is penta-coordinated with apical oxygen.  $\text{Cu}^{2+}$  is ligated via 3 and 4 nitrogen ligands in the equatorial plane for GHK and DAHK, respectively. In GHK,  $\text{Cu}^{2+}$  is coordinated via N-terminal amino nitrogen, the deprotonated amide nitrogen of the first peptide linkage (between glycine and histidine), and the N of the imidazole ring of the histidine resulting in two fused chelate rings with 5 and 6 members. The fourth equatorial position and the axial position are both occupied by O-carboxylate groups of lysine of a neighboring complex. In DAHK,  $\text{Cu}^{2+}$  is coordinated via N-terminal amino nitrogen, the two deprotonated amide nitrogen atoms, and the nitrogen of the imidazole ring of the histidine, resulting in 3 fused chelate rings with 5, 5, and 6 members. The axial position is occupied by a water molecule. In Scheme 2a, the complex with Gly-His-Glu (GHE) shows that copper is ligated via three nitrogen atoms of the same ligand in the equatorial plane ( $\text{NH}_2$ ,  $\text{N}^-$ , and imidazolate N) and has two fused chelate rings (5- and 6-membered), leaving the fourth equatorial position free to be occupied by an oxygen

Scheme 2. Structures of Copper Complexes for Tripeptide Ligands Containing H and E or G at the Central Position



from a water molecule or a neighboring ligand, which is a coordination structure similar to that of GHK. The structure of Cu-EGH (Scheme 2c) shows that the copper is coordinated via 4 nitrogen atoms of the same ligand in the equatorial plane ( $\text{NH}_2$ ,  $\text{N}^-$ ,  $\text{N}^-$ , and imidazolate N) and has three fused chelate rings (5, 5, 6-membered) similarly coordinated to DAHK.

The selected GEMANOVA model for both the most protonated species  $\text{CuH}_{\text{max}}\text{L}$  and the monoprotonated species  $\text{CuHL}$  was the same as that of  $\text{CuH}_{\text{sat}}\text{L}$ : a two-term model describing an interaction between the central and the C-terminal residues ( $e_j f_k$ ), plus an isolated main effect of the N-terminal residue ( $a_i$ ). The preferred model for both  $\text{CuH}_{\text{max}}\text{L}$  and  $\text{CuHL}$  also predicted that N-terminal Glu, central His, and C-terminal Glu promoted greater  $\log\beta$  values; thus, Glu-His-Glu has the greatest  $\log\beta$ . This may be expected, as the presence of Glu (and moreover with poly-Glu residues) allows the formation of polyprotonated species and increases their  $\log\beta$  values and the presence of His at position 2 is known to greatly enhance the stability of  $\text{CuH}_{-1}\text{L}$  species by decreasing the  $\text{pK}_a$  of the first amide proton and suppressing the deprotonation of the second amide group. The complete results are provided in the Supporting Information.

Modeling of the formation of species ( $\text{CuL}$ ) as  $\log\beta(\text{CuL}) - \log\beta(\text{HL})$ , with values of  $\log\beta(\text{HL})$  obtained from our previous study,<sup>7</sup> was of comparable quality to model fittings reported above. The selected GEMANOVA model was a two-term model, describing an interaction between the N-terminal and central residues plus an isolated main effect of the C-terminal residue. The model also showed that having Gly at the N-terminus and center and His at C-terminus results in the lowest

$\text{pK}_a$  of the  $\text{CuL}$  species. The results are shown in the Supporting Information.

Acid dissociation constants of the first ( $\text{pK}_a(\text{CuL})$ ) and second ( $\text{pK}_a(\text{CuH}_{-1}\text{L})$ ) amide groups were calculated by subtracting  $\log\beta(\text{CuH}_{-1}\text{L})$  from  $\log\beta(\text{CuL})$  and subtracting  $\log\beta(\text{CuH}_{-2}\text{L})$  from  $\log\beta(\text{CuH}_{-1}\text{L})$ , respectively (see Table 1).  $\text{pK}_a(\text{CuH}_{-1}\text{L})$  was modeled to determine the pH at which the copper coordination plane (the four equatorial positions) will be saturated or occupied by the peptide donor atoms. The selected GEMANOVA model was the same as that of  $\text{CuH}_{\text{sat}}\text{L}$ : it had two terms describing an interaction between the central and the C-terminal residues ( $e_j f_k$ ), plus an isolated main effect of the N-terminal residue ( $a_i$ ). The model values are shown in Figure 6 and may be interpreted by considering which combination of parameters lead to the lowest  $\text{pK}_a$  values and therefore describes the peptide that gives the most stable

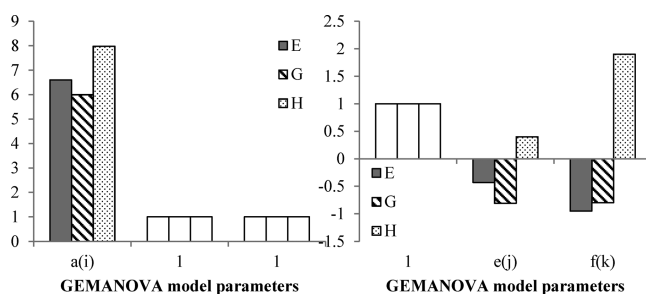


Figure 6. Parameters of the selected GEMANOVA model of  $\text{pK}_a(\text{CuH}_{-1}\text{L})$ . Solid bar, Glu (E); striped bar, Gly (G); dotted bar, His (H).



complex at the most acidic pH. It also indicates that having Gly at the N-terminus and central position and His at the C-terminus will lessen the  $pK_a$  of the amide group of the tripeptide, therefore Gly-Gly-His will saturate the copper coordination plane at the most acidic pH (around 4.4).

## CONCLUSIONS

We report  $\log\beta$  values for 27 complexes between  $Cu^{2+}$  and tripeptides comprising all combinations Glu/Gly/His-Glu/Gly/His-Glu/Gly/His measured by fitting potentiometric titration data. Values of  $\log\beta$  of the complex in which the copper equatorial plane is saturated with ligands, most protonated, monoprotonated,  $\log\beta(CuL) - \log\beta(HL)$ , and  $pK_a$  of the amide group have been modeled by GEMANOVA. The resulting model of the saturated copper species is governed by the interactions between the central and C-terminal residues plus a separate term for the N-terminal residue. It also revealed that the presence of His at the central position controls the copper coordination mode and the complex geometry (two fused or three chelate rings species). The resulting models showed that the formation of both the most and monoprotonated copper species was the same as that of the saturated copper species (i.e., interactions between the central and C-terminal residues plus a separate term for the N-terminal residue). His-His-Glu, followed by Gly-His-His then Glu-His-Glu, was found to be the most efficient ligand for capturing copper in acidic media, with copper complexation starting below pH 3. Glu-His-Glu, followed by Glu-His-His then His-His-Glu, showed the highest fraction of copper bound at pH 7, and Glu-His-His, followed by Glu-His-Glu and His-His-Glu, showed the highest fraction of copper bound at pH 10. Modeling of the  $pK_a$  values of the amide protons was also the same as that of the saturated copper species (a two-term model describing the interaction between the central and C-terminal residues plus an isolated main term describing the main effect of the N-terminus residue). Gly-Gly-His saturates the copper coordination plane at the most acidic pH (pH around 4.4) compared to other peptide ligands. Consequently, the best ligand for binding copper depends on the particular application, whether it is to detect the presence of copper with most sensitivity, to form the most stable species, or to capture the greatest amount of copper. The formation constants are all strongly pH-dependent and controlled by the interactions between the residues of the tripeptide.

## ASSOCIATED CONTENT

### Supporting Information

Schematic representation of experimental design of tripeptide residues with the possible tripeptide combinations formed from Glu, Gly and His; bibliography of  $\log\beta$  and  $pK_a$  values for complexes between copper and tripeptides featured in this paper; titration curves for copper with the 27 tripeptides; GEMANOVA models for  $\log\beta$  for the saturated protonated complexes, most protonated complexes, monoprotonated complexes,  $\log\beta(CuL) - \log\beta(HL)$ , and  $pK_a(CuH_{-1}L)$ ; visible spectra of complexes with HHE, HHH, HGH, and GHE, including PCA decomposition and spectra and relative concentrations of components. This material is available free of charge via the Internet at <http://pubs.acs.org>.

## AUTHOR INFORMATION

### Corresponding Author

\*E-mail: B.Hibbert@unsw.edu.au.

## Notes

The authors declare no competing financial interest.

## ACKNOWLEDGMENTS

The authors acknowledge the considerable help given by Prof. Kip Powell concerning measurement and interpretation of  $\log\beta$  and  $pK$  values. Prof. Powell also provided the IUPAC archive of values<sup>23</sup> that are given in the Supporting Information.

## REFERENCES

- (1) (a) Fenton, D. E.; Okawa, H. *Perspectives on Bioinorganic Chemistry*. JAI Press: London, 1993. (b) Kozłowski, H.; Bal, W.; Dyba, M.; Kowalik-Jankowska, T. *Coord. Chem. Rev.* **1999**, *184*, 319–346. (c) Tian, Z. Q.; Bartlett, P. A. *J. Am. Chem. Soc.* **1996**, *118* (5), 943–949. (d) Burger, K.; Hirose, J.; Kidani, Y.; Kiss, T. L.; Lönnberg, H.; Nagy, L. A.; Noszá, B.; Sóvágó, I. L. *Biocoordination chemistry: Coordination equilibria in biologically active systems*. Burger, K., Ed. Ellis Horwood: Chichester, U.K., 1990.
- (2) (a) Sigel, H.; Martin, R. *Chem. Rev.* **1982**, *82* (4), 385–426. (b) Sovago, I.; Osz, K. *Dalton Trans.* **2006**, 32, 3841–3854. (c) Sigel, H.; Tribolet, R.; Yamauchi, O. *Comments Inorg. Chem.* **1990**, *9* (6), 305–330. (d) Di Natale, G.; Damante, C. A.; Nagy, Z.; Osz, K.; Pappalardo, G.; Rizzarelli, E.; Sovago, I. *J. Inorg. Biochem.* **2008**, *102* (11), 2012–2019. (e) Osz, K.; Nagy, Z.; Pappalardo, G.; Di Natale, G.; Sanna, D.; Micera, G.; Rizzarelli, E.; Sovago, I. *Chem.—Eur. J.* **2007**, *13* (25), 7129–7143. (f) Kállay, C.; Nagy, Z.; Várnagy, K.; Malandrinos, G.; Hadjiliadis, N.; Sovago, I. *Bioinorg. Chem. Appl.* **2007**, *2007*, 30394. (g) Szilagyi, O.; Osz, K.; Várnagy, K.; Sanna, D.; Suli-Vargha, H.; Sovago, I.; Micera, G. *Polyhedron* **2006**, *25* (16), 3173–3182. (h) Kállay, C.; Várnagy, K.; Malandrinos, G.; Hadjiliadis, N.; Sanna, D.; Sóvágó, I. *Dalton Transactions* **2006**, 38, 4545–4552. (i) Kállay, C.; Várnagy, K.; Micera, G.; Sanna, D.; Sóvágó, I. *J. Inorg. Biochem.* **2005**, *99* (7), 1514–1525.
- (3) (a) Sóvágó, I.; Kállay, C.; Várnagy, K. *Coord. Chem. Rev.* **2012**, *256* (19–20), 2225–2233. (b) Hureau, C.; Dorlet, P. *Coord. Chem. Rev.* **2012**, *256* (19–20), 2175–2187.
- (4) Gurd, F. *Pure Appl. Chem.* **1963**, *6* (1), 49–60.
- (5) (a) Pickart, L.; Freedman, J. H.; Loker, W. J.; Peisach, J.; Perkins, C. M.; Stenkamp, R. E.; Weinstein, B. *Nature* **1980**, *288*, 715–717. (b) Shearer, W. T.; Bradshaw, R. A.; Gurd, F. R.; Peters, T. *J. Biol. Chem.* **1967**, *242* (23), 5451–9. (c) Peters, T.; Blumenstock, F. A. *J. Biol. Chem.* **1967**, *242* (7), 1574.
- (6) Kozłowski, H.; Janicka-Klos, A.; Stanczak, P.; Valensin, D.; Valensin, G.; Kulon, K. *Coord. Chem. Rev.* **2008**, *252* (10–11), 1069–1078.
- (7) Khoury, R. R.; Sutton, G. J.; Hibbert, D. B.; Ebrahimi, D. *Dalton Trans.* **2013**, *42* (8), 2940–2947.
- (8) (a) Saudek, V. *Biopolymers* **1981**, *20* (8), 1625–1633. (b) Gergely, A.; Farkas, E., Studies on transition-metal-peptide complexes. Part 6. Influence of side-chain donor group on the equilibrium and thermodynamics of binary and ternary copper(II)-dipeptide complexes. *J. Chem. Soc., Dalton Trans.* **1982**, (2), 381–386; (c) Kállay, C.; Sovago, I.; Várnagy, K. *Polyhedron* **2007**, *26* (4), 811–817. (d) Nagypal, I.; Gergely, A. Studies on transition-metal-peptide complexes. Part 2. Equilibrium study of the mixed complexes of copper(II) with aliphatic dipeptides and amino-acids. *J. Chem. Soc., Dalton Trans.* **1977**, (11), 1109–1111.
- (9) Luczkowski, M.; Kozłowski, H.; Legowska, A.; Rolka, K.; Remelli, M. *Dalton Trans.* **2003**, No. 4, 619–624.
- (10) (a) Trapaidze, A.; Hureau, C.; Bal, W.; Winterhalter, M.; Faller, P. *JBIC, J. Biol. Inorg. Chem.* **2012**, *17* (1), 37–47. (b) Hureau, C.; Eury, H.; Guillot, R.; Bijani, C.; Sayen, S.; Solari, P. L.; Guillon, E.; Faller, P.; Dorlet, P. *Chem.—Eur. J.* **2011**, *17* (36), 10151–10160. (c) Pickart, L.; Lovejoy, S. *Methods Enzymology* **1987**, *147*, 314–328.
- (11) Bro, R.; Jakobsen, M. *J. Chemom.* **2002**, *16* (6), 294–304.
- (12) Yokoyama, A.; Aiba, H.; Tanaka, H. *Bull. Chem. Soc. Jpn.* **1974**, *47* (1), 112–117.

- (13) Braibanti, A.; Ostacoli, G.; Paoletti, P.; Pettit, L.; Sammartano, S. *Pure Appl. Chem.* **1987**, *59*, 1721–1728.
- (14) Yamauchi, O.; Odani, A. *Pure Appl. Chem.* **1996**, *68* (2), 469–496.
- (15) Sjöberg, S. *Pure Appl. Chem.* **1997**, *69*, 1549–1570.
- (16) Gans, P.; Alderighi, L.; Ienco, A.; Peters, D.; Sabatini, A.; Vacca, A. *Coord. Chem. Rev.* **1999**, *184*, 311–318.
- (17) Gans, P.; Sabatini, A.; Vacca, A. *Talanta* **1996**, *43* (10), 1739–1753.
- (18) Kállay, C.; Várnagy, K.; Malandrinos, G.; Hadjiliadis, N.; Sanna, D.; Sóvágó, I. *Dalton Trans.* **2006**, No. 38, 4545–4552.
- (19) (a) Myari, A.; Malandrinos, G.; Deligiannakis, Y.; Plakatouras, J. C.; Hadjiliadis, N.; Nagy, Z.; Sóvágó, I. *J. Inorg. Biochem.* **2001**, *85* (4), 253–261. (b) Farkas, E.; Sovago, I.; Kiss, T.; Gergely, A. *Dalton Trans.* **1984**, No. 4, 611–614. (c) Sanna, D.; Agoston, C. G.; Sovago, I.; Micera, G. *Polyhedron* **2001**, *20* (9–10), 937–947. (d) Aiba, H.; Yokoyama, A.; Tanaka, H. *Bull. Chem. Soc. Jpn.* **1974**, *47* (6), 1437–1441. (e) Aiba, H.; Yokoyama, A.; Tanaka, H. *Bull. Chem. Soc. Jpn.* **1974**, *47* (4), 1003–1007. (f) Aiba, H.; Yokoyama, A.; Tanaka, H. *Bull. Chem. Soc. Jpn.* **1974**, *47* (1), 136–142. (g) Deschamps, P.; Kulkarni, P. P.; Gautam-Basak, M.; Sarkar, B. *Coord. Chem. Rev.* **2005**, *249* (9–10), 895–909.
- (20) Farkas, E.; Sovago, I.; Kiss, T.; Gergely, A. *J. Chem. Soc., Dalton Trans.* **1984**, No. 4, 611–614.
- (21) Bóka, B.; Myari, A.; Sóvágó, I.; Hadjiliadis, N. *J. Inorg. Biochem.* **2004**, *98* (1), 113–122.
- (22) Huang, H.; Chaudhary, S.; Van Horn, J. D. *Inorg. Chem.* **2005**, *44* (4), 813–815.
- (23) Pettit, L. D.; Powell, K. J. *Stability Constants Database (SC-Database)*, Release 5.8; IUPAC, Academic Software: Otley, U.K., 2010.